

Multimodal 3D Reasoning Segmentation with Complex Scenes

Xueying Jiang¹ Lewei Lu² Ling Shao³ Shijian Lu^{1*}

¹S-Lab, Nanyang Technological University, Singapore

²Sensetime Research, China

³UCAS-Terminus AI Lab, University of Chinese Academy of Sciences, China

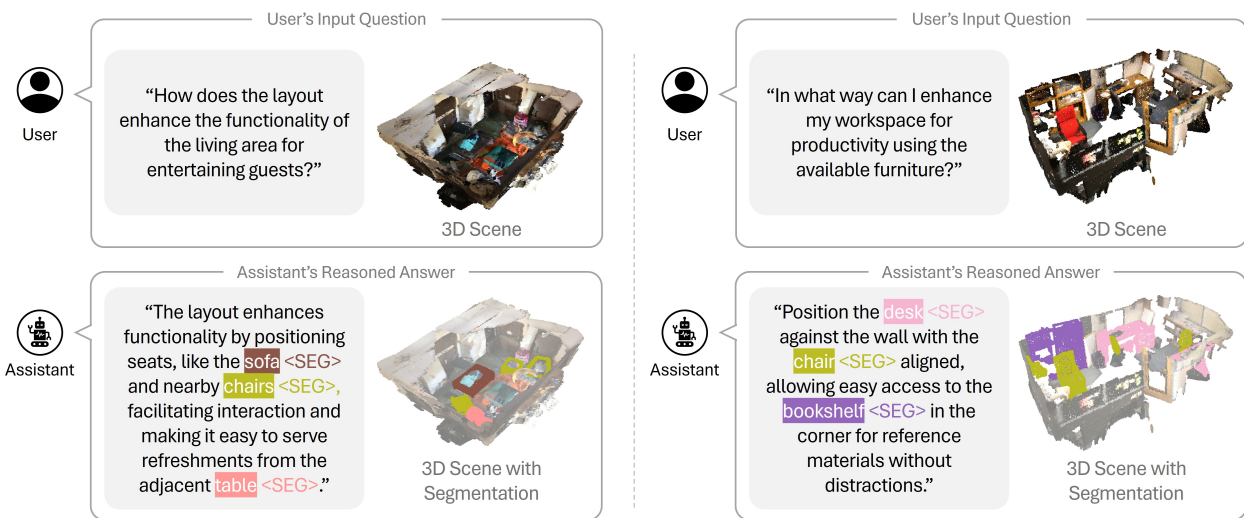


Figure 1. The proposed MORE3D enables multi-object reasoning segmentation for 3D scenarios. It can comprehend the intention behind user questions, handle complex 3D scenes with multiple objects, and produce fine-grained explanations with 3D spatial relations among objects, demonstrating strong reasoning and 3D segmentation capabilities.

Abstract

The recent development in multimodal learning has greatly advanced the research in 3D scene understanding in various real-world tasks such as embodied AI. However, most existing work shares two typical constraints: 1) they are short of reasoning ability for interaction and interpretation of human intention and 2) they focus on scenarios with single-category objects only which leads to over-simplified textual descriptions due to the negligence of multi-object scenarios and spatial relations among objects. We bridge the research gaps by proposing a 3D reasoning segmentation task for multiple objects in scenes. The task allows producing 3D segmentation masks and detailed textual explanations as enriched by 3D spatial relations among objects. To this end, we create ReasonSeg3D, a large-scale and high-quality benchmark that integrates 3D seg-

mentation masks and 3D spatial relations with generated question-answer pairs. In addition, we design MORE3D, a novel 3D reasoning network that works with queries of multiple objects and tailored 3D scene understanding designs. MORE3D learns detailed explanations on 3D relations and employs them to capture spatial information of objects and reason textual outputs. Extensive experiments show that MORE3D excels in reasoning and segmenting complex multi-object 3D scenes, and the created ReasonSeg3D offers a valuable platform for future exploration of 3D reasoning segmentation. The dataset and code will be released.

1. Introduction

With the recent advancements in deep learning, 3D scene understanding has become one key component in various

real-world tasks such as embodied AI and autonomous driving. The capabilities of understanding spatial relations among 3D objects in scenes and grasping the intention of human users have become essential for machines for interpreting 3D scenes, interacting with 3D objects in scenes, and achieving various complex and real-world missions while navigating within 3D environments.

On the other hand, most existing 3D scene understanding work does not possess reasoning and interpretation abilities for interacting with user textual inputs. For example, several work introduces foundation models such as large language models (LLMs) to empower 3D scene understanding on captioning [4, 7, 14], question answering [2, 11, 14, 27, 30], visual grounding [5, 10, 14, 18, 20, 45, 53], and referring [17, 33, 40, 49], but they are short of reasoning capabilities for deducting human intentions. Recently, several studies attempt to introduce the reasoning ability of LLMs into 3D scene understanding tasks. However, they mostly focus on segmenting single or single-category objects but cannot handle complex scenes with multiple objects of different categories [5, 13, 16]. Hence, they cannot understand 3D spatial relations among objects and produce fine-grained textual explanations, hampering their applications in various real-world scenarios that often come with multiple objects of different categories.

We propose a multi-object 3D reasoning segmentation task that can produce 3D segmentation masks and textual explanations with rich 3D spatial relations among objects in scenes, given 3D scenes and user questions as inputs. To this end, we create ReasonSeg3D, a large-scale and high-quality benchmark that can evaluate 3D reasoning segmentation with multiple 3D objects and rich spatial relations among them. Different from prior 3D reasoning segmentation benchmarks [13, 16], ReasonSeg3D expands the scope into multi-object space which is well aligned with real-world tasks that often come with multiple objects. In addition, ReasonSeg3D integrates 3D spatial information into question-answer pairs, where the 3D spatial relations in textual answers benefit 3D reasoning segmentation clearly.

On top of ReasonSeg3D, we design *MORE3D*, a simple yet effective technique that enables multi-object reasoning segmentation with textual explanations to users' questions. Specifically, MORE3D extracts object-specific point cloud embedding for precise prediction of multi-category objects in complex 3D scenes. It incorporates textual explanations with detailed 3D spatial relations of multiple objects in answers, guiding the model toward a comprehensive understanding of 3D scenes. The generated textual answers support accurate segmentation and comprehensive reasoning for complex 3D scenes. As illustrated in Figure 1, MORE3D demonstrates strong reasoning capability for comprehending the intention behind user's input questions and complex 3D scenes, producing accurate 3D seg-

mentation and explanatory answers with respect to multiple 3D objects in scenes.

The major contributions of this work can be summarized in three aspects. First, we introduce a new multi-object 3D reasoning segmentation task, together with a large-scale and high-quality benchmark that incorporates 3D spatial relations for effective evaluations of multi-object 3D reasoning segmentation. Second, we design a reasoning segmentation technique that can handle multi-object 3D reasoning segmentation and produce fine-grained textual explanations with 3D spatial relations among objects in scenes. Third, extensive experiments demonstrate the superiority of our proposed multi-object reasoning segmentation technique as well as the validity of our created benchmark on multi-object 3D reasoning segmentation.

2. Related Work

2.1. Language-Instructed 3D Tasks

Integrating point clouds with natural language processing has widespread applications, drawing increasing interest in language-instructed 3D scene understanding. Existing language-instructed 3D scene understanding methods can be broadly grouped into two categories. The first category focuses on 3D segmentation [3, 9, 17, 19, 26, 29, 33, 40, 44, 46, 49], such as OpenScene [31], Openmask3D [36], 3D-STMN [41], which produce segmentation masks but lack reasoning abilities and textual or conversational output. This limits their ability to comprehend the user's intention and interact with the user in real-world applications. The second category focuses on tasks such as 3D captioning [4, 7, 14], 3D question answering [2, 11, 14, 27, 30], and visual grounding [5, 10, 14, 18, 20, 45, 53]. They can generate textual outputs like phrases or conversational outputs, but leave the fine-grained segmentation task untouched and have no reasoning ability either. Different from existing methods, the proposed MORE3D predicts textual answers with explanation and accurate segmentation of multiple 3D objects within complex scenes, demonstrating strong reasoning capability in comprehending the intention behind the user's input questions.

2.2. Reasoning Segmentation

Reasoning Segmentation is first introduced by LISA [23] to generate segmentation masks from complex, implicit textual queries. Specifically, LISA integrates LLaVA [25] with SAM, enhancing segmentation through the vision-language model's reasoning capabilities. Following LISA, PixelLM [34] improves pixel-level reasoning segmentation using multimodal models with a lightweight decoder and segmentation codebook, LLM-Seg [38] bridges the Segmentation Anything Model and LLMs by selecting mask proposals, and LLaVASEg [47] incorporates query-focused

segmentation into large language models where chain-of-thought prompting is adopted to preserve dialogue functions. In addition, VISA [43] extends reasoning segmentation to video by combining multimodal language models with a mask decoder, facilitating complex video segmentation from implicit text queries and world knowledge. In the 3D domain, PARIS3D [21] and Reasoning3D [6] focus on part segmentation with explanations for individual 3D objects, leaving 3D segmentation of complex scenes untouched. Recent studies like SegPoint [13] and Reason3D [16] integrate LLMs’ reasoning ability into 3D segmentation, but they are limited to segmentation for single-category objects and have no textual explanations. In contrast, our approach targets multi-object 3D segmentation and provides textual explanations in the output answer, enhancing the model’s understanding of 3D spatial relations and offering a more practical solution for real-world complex scenes.

2.3. Large Multimodal Models

Inspired by the remarkable learning ability of Large Language Models (LLMs), recent research has expanded into the visual domain and developed a series of Large Multimodal Models (LMMs) [1, 50]. The prevalent approach focuses on aligning visual representations with the linguistic embeddings of LLMs. For example, BLIP-2 [24] and mPLUG-OWL [48] encode image features with a visual encoder, integrating them into the LLMs with text embeddings. LLaVA [25] and MiniGPT4 [52] align image-text features followed by instruction tuning, and they also explore image retrieval for LLMs. Recent studies delve into the integration of multimodal LLMs with vision tasks. For example, VisionLLM [39] provides an interface for vision-centric tasks via instruction tuning though it does not exploit LLMs for complex reasoning. VisionLLM-v2 [42] integrates visual perception, understanding, and generation within a unified framework by using a “super link” to connect the multimodal large model with task-specific decoders. DetGPT [32] introduces multimodal LLMs into open-vocabulary detectors for instruction-based detection tasks. GPT4RoI [51] introduces spatial boxes as inputs, training on region-text pairings. LISA [23] enhances segmentation in multimodal LLMs by introducing a <SEG> token. These existing studies primarily target downstream tasks in the 2D domain. In contrast, our approach extends into the 3D domain to enable multi-object segmentation of 3D point clouds and provides textual explanations to support reasoning in the segmentation process.

3. ReasonSeg3D Dataset

Most existing reasoning segmentation datasets are not suitable for studying the proposed 3D multi-object reasoning segmentation task. Specifically, existing reasoning segmen-

tation datasets have two critical limitations. First, the existing 2D reasoning segmentation datasets [23, 34, 38, 43] lack 3D data, making them unsuitable for 3D tasks. Second, the existing 3D reasoning datasets [13, 16] focus on single-category objects as illustrated in Table 1, and they contain only a few hundred scenes which are far fewer than standard 3D segmentation datasets [8, 35]. Additionally, these 3D reasoning datasets lack textual explanations with spatial information, hindering them from training MLLMs for better 3D spatial relation understanding. We bridge this gap by proposing a data generation pipeline as well as a new 3D reasoning segmentation dataset ReasonSeg3D, more details to be elaborated in the following subsections.

3.1. Dataset Definition

In the proposed ReasonSeg3D, each point cloud P is paired with multiple $\{x_{que}, y_{ans}, M\}$ triplets, where x_{que} is a question targeting one or more objects in the image, y_{ans} is the textual answer containing the explanation for the reasoning segmentation, and M represents the 3D segmentation masks corresponding to y_{ans} . The question x_{que} is designed to require world knowledge and reasoning ability to accurately identify and segment multiple objects. For example, instead of directly asking “Where are the sofa and table?”, ReasonSeg3D formulates the question by “Where would be the most suitable place for reading a book in this layout?”. An answer y_{ans} in ReasonSeg3D is constructed to involve multiple objects, and it also include explanations with 3D spatial relations. For example, the y_{ans} to the above question is formulated by “The corner with the sofa and a small table next to it can serve as a perfect reading nook, providing comfort and a quiet atmosphere.”.

3.2. Dataset Generation Pipeline

Several reasoning segmentation datasets [23, 38] employ LLaVA [25] for image captioning and text-only GPT-4 to produce question-answer pairs according to the generated captions. However, GPT-4 cannot understand the image content well and its generated question-answer pairs often lack crucial 3D spatial relations that are essential for 3D reasoning segmentation in various real-world tasks.

We design a novel data generation pipeline that introduces GPT-4o that possesses superior visual content understanding capabilities. The pipeline allows generating more practical questions and answers by incorporating spatial relations among objects in scenes. Specifically, we employ both scene image and its ground-truth segmentation to enhance GPT-4o’s 3D spatial understanding capabilities. The prompt template is structured in two parts: the first part contains basic requirements for the GPT-4o and the sec-

Basic Requirements

Your task is to create questions and corresponding answers based on a given image, with the original indoor scene image on the left and corresponding segmentation ground-truth on the right. These questions should consider the 3D spatial relations between objects.

Requirements for Questions and Answers

Make sure your generated questions and answers fulfill requirements:

1. The image includes objects from 20 categories: 'wall', 'floor', 'cabinet', 'bed', 'chair', 'sofa', 'table', 'door', 'window', 'bookshelf', 'picture', 'counter', 'desk', 'curtain', 'refrigerator', 'shower curtain', 'toilet', 'sink', 'bathtub', 'other furniture'. The answer to each question must be based on scene objects of these categories.
2. It's good to inquire about a complete activity in the question.
3. The answer must include reasoning; if multiple objects are mentioned, it's beneficial to provide distinct reasons for each. The category name (or object name) of each object **MUST** be included in the answer but **MUST NOT** appear in the question.
4. Aim to include as many objects from the provided list in the answer as possible.
5. Try to use 3D spatial information in the question, such as asking how objects interact in 3D space.

(a)



Input Image of a 3D Scene



Ground-Truth Segmentation

Question: “How can I make this space more inviting for a casual chat?”

Answer: “You can position the **comfortable sofa** <SEG> and **chairs** <SEG> close to the **coffee table** <SEG>, ensuring that everyone has a convenient spot to place their drinks or personal items, fostering a relaxed and interactive setting.”

(b)

Figure 2. Illustration of the prompt template in our dataset generation. (a) One example prompt template in our dataset generation on 3D multi-object reasoning. (b) With a sample input image to GPT-4o and the corresponding ground-truth segmentation on the top, the two boxes below present one generated question-answer pair where text of different colors highlights different objects.

Dataset	Venue	Scale		Data for Each QA Pair			
		# Scene	# QA Pair	Single Object	Multiple Objects	Multiple Categories	Explanation
Instruct3D [13]	ECCV 2024	280	2,565	✓	✓	✗	✗
Reason3D [16]	arXiv	N/A	2,484	✓	✗	✗	✗
ReasonSeg3D (Ours)	-	1,513	20,113	✓	✓	✓	✓

Table 1. Comparison of existing 3D scene-level reasoning segmentation datasets. ReasonSeg3D stands out for its large-scale, high-quality data, supporting segmenting multiple 3D objects across multiple categories and offering explanations with 3D spatial relations.

ond specifies detailed requirements for generating questions and answers with a focus on describing 3D spatial relations among objects. With this template, GPT-4o autonomously selects objects to form question-answer pairs that reflect the scene’s content and spatial layout. On top of that, we conduct human verification to ensure the quality of the generated question-answer pairs. Figure 2 shows one example of the designed prompt template and one question-answer pair generated by using the template.

3.3. Dataset Statistics

ReasonSeg3D comprises 1513 scenes and 20,113 data samples in total, with point clouds sourced from ScanNetv2 [8]. Following [8], we divide ReasonSeg3D into training and validation sets, comprising 1201 and 312 scenes, respec-

tively. In the generated dataset, each scene has 13.3 questions on average. The dataset contains 20 different object categories for segmentation.

4. Method

4.1. Task Definition

Multi-object 3D reasoning segmentation takes a single point cloud P and input user questions X_{que} as input, aiming to reason the implicit intention behind X_{que} and produce textual answers \hat{Y}_{ans} including explanations and 3D segmentation masks \hat{M} of multiple objects in P .

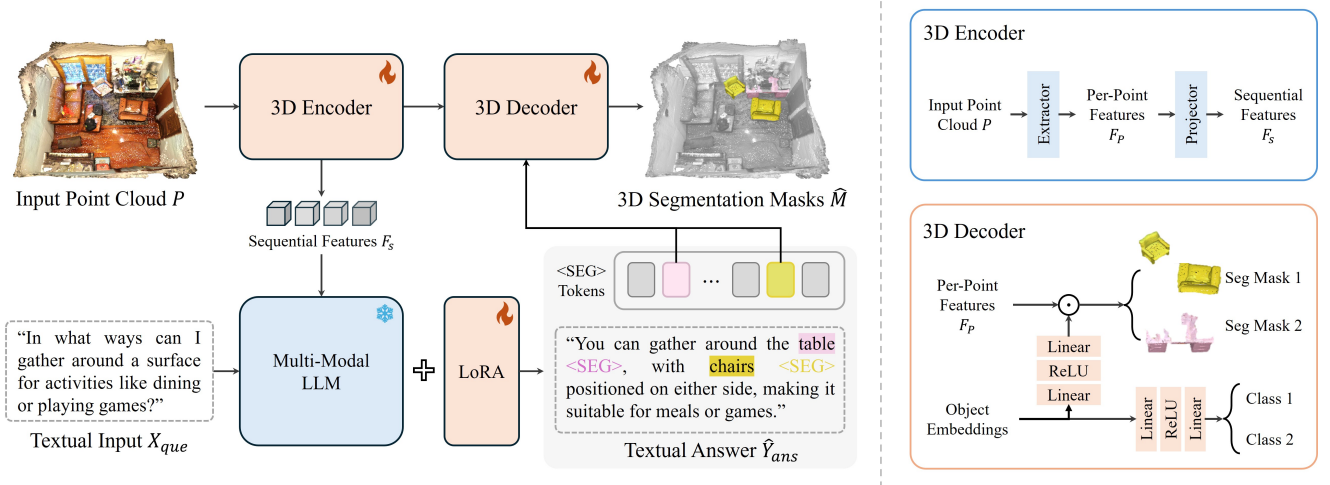


Figure 3. Overview of our proposed MORE3D: Given an input point cloud, the 3D Encoder first extracts per-point features F_p and projects them into sequential features F_s . The sequential features F_s , together with the textual input X_{que} , are then fed into a multimodal LLM to perform reasoning, producing textual answers \hat{Y}_{ans} with both detailed explanations and descriptions of 3D spatial relationships among multiple objects. Finally, embeddings for multiple $\langle \text{SEG} \rangle$ tokens and the per-point features are passed to the 3D Decoder to produce 3D segmentation masks and classification results. The module marked with a snowflake icon is frozen during training, while those marked with a flame icon are trainable.

4.2. Overall Framework

Figure 3 shows the framework of the proposed MORE3D which enables **Multi-Object 3D Reasoning** segmentation and provides textual Explanations based on the user’s input question. Given an input point cloud P , the 3D Encoder first extracts per-point features F_p and then projects F_p into sequential features F_s that can be processed by LLMs. The sequential features F_s and input text queries are processed by the LLM, generating textual answers \hat{Y}_{ans} that include textual explanations \hat{Y}_{text} and multi-object $\langle \text{SEG} \rangle$ tokens $\hat{Y}_{\langle \text{SEG} \rangle}$. The $\langle \text{SEG} \rangle$ tokens $\hat{Y}_{\langle \text{SEG} \rangle}$ indicate the request for 3D segmentation masks, and the corresponding object embeddings F_{seg} are extracted from the LLM’s embeddings. These object embeddings F_{seg} are further combined with the per-point features F_p within the 3D Decoder by dot product, ensuring that the object-specific information interacts with the overall point cloud features to generate the final 3D segmentation masks \hat{M} and classification predictions.

4.3. Multi-Object 3D Reasoning Segmentation

We design an object-specific point cloud embedding extraction approach to achieve the multi-object 3D reasoning segmentation. The embedding extraction approach enables precise segmentation and reasoning for multiple objects of different categories in complex point clouds, integrating the LLM with a 3D point cloud decoder to generate segmentation masks and textual explanations.

The LLM takes point cloud features F_s and text queries X_{que} as input, generating textual answers \hat{Y}_{ans} , which

include textual explanations \hat{Y}_{text} and multi-object $\langle \text{SEG} \rangle$ tokens $\hat{Y}_{\langle \text{SEG} \rangle}$. Specifically, each output textual answer consists of a paragraph of textual explanations accompanied by a set of $\langle \text{SEG} \rangle$ tokens, where the number of $\langle \text{SEG} \rangle$ tokens equals the number of 3D objects indicated in the input text query. In each answer, the 3D object’s name is followed by a $\langle \text{SEG} \rangle$ token. For example, the LLM might generate the following answer: “You can use the spacious sofa $\langle \text{SEG} \rangle$ for seating, positioned near a central table $\langle \text{SEG} \rangle$ for drinks and snacks, while additional chairs $\langle \text{SEG} \rangle$ provide extra seating options for guests.” Each $\langle \text{SEG} \rangle$ token indicates a request for a point cloud segmentation mask.

Object-Specific Point Cloud Embeddings Extraction.

After obtaining the multi-object $\langle \text{SEG} \rangle$ tokens $\hat{Y}_{\langle \text{SEG} \rangle}$ in the output textual answer \hat{Y}_{ans} , we extract the point cloud embeddings generated by the multimodal LLM for each $\langle \text{SEG} \rangle$ token and feed them into the 3D Decoder to generate the corresponding segmentation masks. As illustrated in Figure 4, each point cloud P is associated with N textual answers \hat{Y}_{ans} , and we illustrate the process with one textual answer \hat{Y}_{ans}^n for clarity. The LLM’s textual answer includes multiple $\langle \text{SEG} \rangle$ tokens, and we use a multi-seg index list I_{seg} to record the positions of these tokens in the tokenized output. I_{seg} is obtained from the ground-truth answer y_{ans}^n during training, and the predicted answer \hat{Y}_{ans}^n during infer-

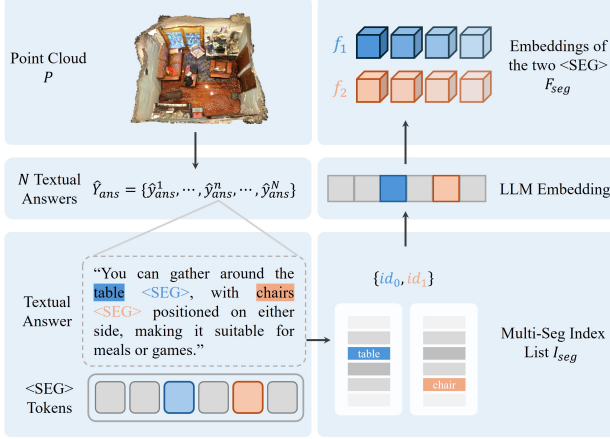


Figure 4. Extraction of object-specific point cloud embeddings. Each predicted textual answer contains multiple $<\text{SEG}>$ tokens, with their positions recorded in a multi-segment index list I_{seg} . The LLM embedding corresponding to each $<\text{SEG}>$ token is extracted based on the multi-segment index list for obtaining object-specific point cloud embeddings.

ence. The multi-seg index list I_{seg} is defined by:

$$I_{seg} = \{id_0, id_1, \dots, id_S\}, \quad (1)$$

where S denotes the number of $<\text{SEG}>$ tokens in the textual answer. I_{seg} is then used to retrieve the corresponding point cloud embeddings F_{seg} from the LLM's hidden states. The process can be formulated as follows:

$$F_{seg} = \{f_i, i \in I_{seg}\}, \quad (2)$$

where f_i is the i -th point cloud embeddings in the LLM's hidden states.

For the example in Figure 4, the 3rd and 5th hidden embeddings corresponding to the table and chair are extracted, matching the first and second $<\text{SEG}>$ tokens in the answer. Each $<\text{SEG}>$ token corresponds to a 3D object in \hat{Y}_{ans}^n , allowing us to obtain the point cloud embeddings from the LLM for subsequent segmentation.

4.4. Explainability

The LLM-generated textual answers \hat{Y}_{ans} contain explanations of the implicit intention of the user questions. In addition, the answer includes the descriptions of 3D spatial relations of multiple objects which provide useful guidance for identifying these objects. Unlike most existing reasoning-based segmentation methods [13, 16, 38, 43] that just output statements like "It is $<\text{SEG}>$." without further explanation, our generated answer integrates detailed explanations about 3D spatial relations to enhance segmentation. The ground truth answers Y_{ans} also incorporate these 3D spatial relations and are used to supervise the generated output textual answers, guiding the model to capture spatial

information effectively. The textual answer loss is defined by:

$$L_{ans} = CE(Y_{ans}, \hat{Y}_{ans}), \quad (3)$$

where CE denotes the cross-entropy loss.

4.5. Training Objectives

For point cloud segmentation, we optimize each predicted point cloud segmentation mask as follows:

$$L_{mask} = BCE(M, \hat{M}) + DICE(M, \hat{M}), \quad (4)$$

where M denotes the ground truth segmentation mask, \hat{M} denotes the predicted segmentation mask, BCE denotes the binary cross-entropy loss and $DICE$ denotes the Dice loss [28]. We use the cross-entropy loss to supervise the point cloud classification as follows:

$$L_{cls} = CE(C, \hat{C}), \quad (5)$$

where C is the ground truth classification label and \hat{C} is the classification prediction.

The proposed model is trained end-to-end with a textual answer loss L_{ans} for textual answer generation, a mask loss L_{mask} for point cloud segmentation mask prediction, and a classification loss L_{cls} for point cloud classification. The overall loss function is formulated as follows:

$$L = L_{ans} + L_{mask} + L_{cls}. \quad (6)$$

5. Experiment

5.1. Experimental Settings

Evaluation Metrics. Following prior studies on reasoning segmentation [23, 34, 38], we adopt two evaluation metrics including cumulative IoU (cIoU) and generalized IoU (gIoU). cIoU is computed as the cumulative intersection over cumulative union, while gIoU is the average Intersection-over-Union (IoU) across all samples.

Implementation Details. We conduct experiments on one NVIDIA V100 GPU and train the framework for 100 epochs with a batch size of 1. We use the Adam [22] optimizer with the initial learning rate of 1×10^{-4} . We adopt LLaMA-7B [37] as our multimodal LLM backbone and LoRA [15] to perform efficient fine-tuning. All experiments are conducted on the proposed ReasonSeg3D dataset.

5.2. Benchmarking with Existing Methods

We benchmark MORE3D with state-of-the-art 3D segmentation and vision-language methods on the ReasonSeg3D validation set. As Table 2 shows, our method achieves superior reasoning segmentation performance across all evaluation metrics. Specifically, OpenScene [31], PLA [9], and RegionPLC [46] are designed to comprehend input words

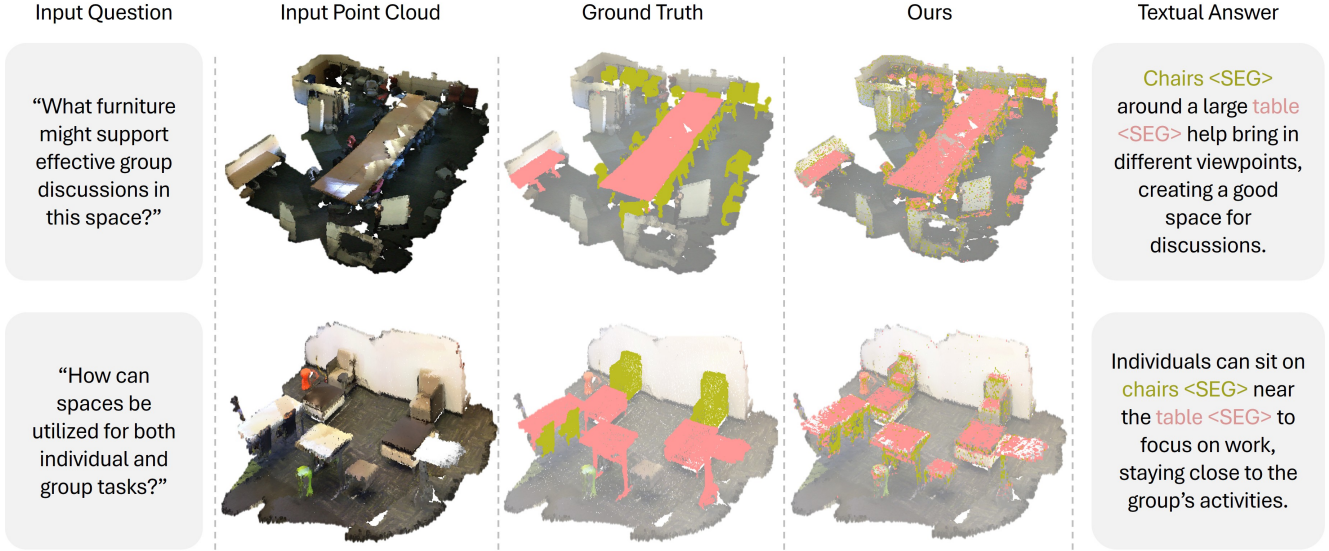


Figure 5. Segmentation visualization over the ReasonSeg3D validation set. Each case presents a user input question, the corresponding input point cloud, the ground-truth segmentation, and the prediction by the proposed MORE3D. Best viewed in color and zoom-in. Green indicates chairs, and pink indicates tables. Best viewed in color.

Method	Venue	cIoU	gIoU
3D Segmentation Methods			
OpenScene [31]	CVPR 23	7.69	9.52
PLA [9]	CVPR 23	10.76	10.27
RegionPLC [46]	CVPR 24	10.82	11.06
3D-STMN [41]	AAAI 24	19.37	20.70
RefMask3D [12]	MM 24	20.53	22.81
MDIN [40]	MM 24	23.04	23.49
3D Vision-Language Methods			
3D-LLM [14]	NeurIPS 23	21.36	22.49
3D-VisTA [53]	ICCV 23	<u>23.95</u>	<u>24.77</u>
MORE3D (Ours)	-	30.19	32.01

Table 2. Benchmarking on the ReasonSeg3D validation set with evaluation metrics cIoU and gIoU. Best in **bold**, second underlined.

or phrases based on CLIP-based language models. They lack the ability to reason user intention from input questions and to correctly generate answers targeting at corresponding multiple objects. Consequently, the predicted 3D segmentation masks by these methods cannot be aligned correctly with ground-truth 3D segmentation masks, resulting in low cIoU and gIoU. Moreover, 3D-STMN [41] and RefMask3D [12] are tailored for single-object segmentation and therefore cannot handle multiple objects, while MDIN [40] exhibits weaker reasoning ability for interpreting implicit human intention. Additionally, 3D-LLM [14] and 3D-VisTA [53], designed for general 3D tasks, are re-implemented on our proposed 3D reasoning segmentation

task for comparison. In contrast, MORE3D can accurately reason the implicit intention of user questions, predicting 3D segmentation masks that are more consistent with the ground truth.

Qualitative Results. Figure 5 presents qualitative segmentation by the proposed MORE3D with two examples from the ReasonSeg3D validation set. Each example demonstrates the user question, input point cloud, ground-truth segmentation, and the 3D segmentation masks that are predicted by MORE3D. We can observe that MORE3D could accurately predict the 3D segmentation masks that are highly aligned with the ground-truth segmentation masks. Specifically, in the example at the top, despite many chairs closely surrounding the central long table, MORE3D can correctly distinguish and segment them. For the example at the bottom, despite the similar appearance and size of tables and chairs, MORE3D can distinguish and segment them precisely. The visualization indicates that MORE3D can comprehend the implicit intention behind the user questions and segment multiple objects accurately.

5.3. Ablation Study

We conduct extensive ablation studies on the ReasonSeg3D validation set to evaluate our designs. Specifically, we examine MORE3D from the aspect of the approach for object-specific point cloud embeddings extraction, the loss design, the point cloud decoding approach, as well as the way of prediction.

Index	Approach	cIoU	gIoU
1	Random	20.30	21.23
2	with I_{seg}	30.19	32.01

Table 3. Ablation study on the approach of object-specific point cloud embeddings extraction. The best results are in **bold**.

Index	L_{ans}	L_{mask}	cIoU	gIoU
1			13.72	14.73
2	✓		15.23	16.14
3		✓	23.30	28.91
4	✓	✓	30.19	32.01

Table 4. Ablation study of the loss functions on the ReasonSeg3D validation set. L_{ans} and L_{mask} refer to the textual answer loss and the point cloud segmentation mask loss, respectively. The best results are in **bold**.

Embedding Extraction. We examine the effectiveness of the designed multi-seg index list I_{seg} for the object-specific point cloud embeddings extraction in MORE3D. As Table 3 shows, using the multi-seg index list I_{seg} can achieve better performance than adopting the random selection approach. This is largely because the LLM’s embeddings corresponding to multiple objects are extracted precisely with the help of I_{seg} . As a comparison, the random selection could extract embeddings unrelated to target objects like “table” or “chairs”, and it could also extract embeddings belonging to irrelevant non-object words, such as “around” and “suitable”. This explains why using the multi-seg index list I_{seg} is more effective for extracting object-specific point cloud embeddings corresponding to multiple target objects.

Loss Functions. We examine the impact of the textual answer loss L_{ans} and the mask loss L_{mask} in Equations 3 and 4, where L_{ans} supervises the textual answers output by the multimodal LLM and L_{mask} supervises the 3D point cloud segmentation prediction. As Table 4 shows, without L_{ans} and L_{mask} , the performance drops greatly due to the lack of supervision from both ground-truth textual answers and segmentation masks, which hinders the model from generating appropriate answers and accurate 3D segmentation masks. When either L_{ans} or L_{mask} is used, the performance improves consistently due to partial supervision from the ground-truth textual answers or the segmentation masks. When both L_{ans} and L_{mask} are employed, the reasoning ability for generating answers and the capability of predicting 3D segmentation masks of MORE3D are both improved by large margins, demonstrating the effectiveness and synergies of the two designed losses.

Index	Operation	cIoU	gIoU
1	Addition	28.26	31.01
2	Concatenation	29.42	31.17
3	Dot Product	30.19	32.01

Table 5. Ablation study on the approach of point cloud decoding operation in the 3D Decoder. The best results are in **bold**.

Index	Manner	cIoU	gIoU
1	Unified	29.06	30.43
2	Separated	30.19	32.01

Table 6. Ablation study on different approaches of prediction in the 3D Decoder. The best results are in **bold**.

Decoding Operation. We examine how different point cloud decoding operations affect 3D reasoning segmentation. Besides the dot product for refined queries and features, we explore addition and concatenation to investigate whether richer point cloud information improves training. As Table 5 shows, the Addition and the Concatenation operations achieve lower performance compared with the Dot Product operation since they either add or concatenate the embeddings of each object with the per-point features of the global scene, introducing abundant features of irrelevant objects and leading to inferior performance. Differently, the Dot Product operation selectively extracts only the relevant features from the per-point features of the global scene by identifying those highly correlated with the object embeddings. This leads to better performance thanks to its extracted object-specific features.

Prediction Approaches. We examine the effectiveness of different prediction approaches including unified and separated approaches for the prediction of 3D segmentation masks and classification. Table 6 shows experimental results. For the unified approach, the 3D segmentation masks and classification results are predicted by a single instead of two separate network branches. This results in lower performance due to the increased learning burden when a single network branch must learn to perform segmentation and classification simultaneously. In contrast, the separate approach as illustrated in the bottom right of Figure 3 assigns each task to an independent network branch to learn. This allows each branch to focus on its respective task which lowers the learning burden and improves performance clearly.

6. Conclusion

This paper presents a novel multi-object 3D reasoning segmentation task, producing both 3D segmentation masks and textual explanations with rich 3D spatial relations among multiple objects within complex 3D scenes. To this end,

we develop ReasonSeg3D, a large-scale benchmark featuring rich 3D spatial relations integrated into question-answer pairs, designed to evaluate multi-object 3D reasoning segmentation effectively. On top of this, we propose MORE3D, a technique for multi-object 3D reasoning segmentation with textual explanations, demonstrating strong reasoning abilities in response to user questions. Extensive experiments validate the effectiveness of MORE3D. Future work will focus on generalizing our work to diverse and challenging 3D environments, such as outdoor scenes, to expand the scope of applications.

References

- [1] Jean-Baptiste Alayrac, Jeff Donahue, Pauline Luc, Antoine Miech, Iain Barr, Yana Hasson, Karel Lenc, Arthur Mensch, Katherine Millican, Malcolm Reynolds, et al. Flamingo: a visual language model for few-shot learning. *Advances in Neural Information Processing Systems*, 35:23716–23736, 2022. 3
- [2] Daichi Azuma, Taiki Miyanishi, Shuhei Kurita, and Motoaki Kawanabe. Scanqa: 3d question answering for spatial scene understanding. In *Proceedings of the IEEE/CVF Conference on Computer Vision and Pattern Recognition*, pages 19129–19139, 2022. 2
- [3] Mohamed El Amine Boudjoghra, Angela Dai, Jean Lahoud, Hisham Cholakkal, Rao Muhammad Anwer, Salman Khan, and Fahad Shahbaz Khan. Open-yolo 3d: Towards fast and accurate open-vocabulary 3d instance segmentation. *arXiv preprint arXiv:2406.02548*, 2024. 2
- [4] Sijin Chen, Hongyuan Zhu, Xin Chen, Yinjie Lei, Gang Yu, and Tao Chen. End-to-end 3d dense captioning with vote2cap-detr. In *Proceedings of the IEEE/CVF Conference on Computer Vision and Pattern Recognition*, pages 11124–11133, 2023. 2
- [5] Sijin Chen, Xin Chen, Chi Zhang, Mingsheng Li, Gang Yu, Hao Fei, Hongyuan Zhu, Jiayuan Fan, and Tao Chen. Ll3da: Visual interactive instruction tuning for omni-3d understanding reasoning and planning. In *Proceedings of the IEEE/CVF Conference on Computer Vision and Pattern Recognition*, pages 26428–26438, 2024. 2
- [6] Tianrun Chen, Chunyan Yu, Jing Li, Jianqi Zhang, Lanyun Zhu, Deyi Ji, Yong Zhang, Ying Zang, Zejian Li, and Lingyun Sun. Reasoning3d-grounding and reasoning in 3d: Fine-grained zero-shot open-vocabulary 3d reasoning part segmentation via large vision-language models. *arXiv preprint arXiv:2405.19326*, 2024. 3
- [7] Zhenyu Chen, Ronghang Hu, Xinlei Chen, Matthias Nießner, and Angel X Chang. Unit3d: A unified transformer for 3d dense captioning and visual grounding. In *Proceedings of the IEEE/CVF International Conference on Computer Vision*, pages 18109–18119, 2023. 2
- [8] Angela Dai, Angel X Chang, Manolis Savva, Maciej Halber, Thomas Funkhouser, and Matthias Nießner. Scannet: Richly-annotated 3d reconstructions of indoor scenes. In *Proceedings of the IEEE/CVF Conference on Computer Vision and Pattern Recognition*, pages 5828–5839, 2017. 3, 4
- [9] Runyu Ding, Jihan Yang, Chuhui Xue, Wenqing Zhang, Song Bai, and Xiaojuan Qi. Pla: Language-driven open-vocabulary 3d scene understanding. In *Proceedings of the IEEE/CVF Conference on Computer Vision and Pattern Recognition*, pages 7010–7019, 2023. 2, 6, 7
- [10] Zoey Guo, Yiwen Tang, Ray Zhang, Dong Wang, Zhigang Wang, Bin Zhao, and Xuelong Li. Viewrefer: Grasp the multi-view knowledge for 3d visual grounding. In *Proceedings of the IEEE/CVF International Conference on Computer Vision*, pages 15372–15383, 2023. 2
- [11] Ziyu Guo, Renrui Zhang, Xiangyang Zhu, Yiwen Tang, Xianzheng Ma, Jiaming Han, Kexin Chen, Peng Gao, Xianzhi Li, Hongsheng Li, et al. Point-bind & point-llm: Aligning point cloud with multi-modality for 3d understanding, generation, and instruction following. *arXiv preprint arXiv:2309.00615*, 2023. 2
- [12] Shuteng He and Henghui Ding. Refmask3d: Language-guided transformer for 3d referring segmentation. In *Proceedings of the ACM International Conference on Multimedia*, pages 8316–8325, 2024. 7
- [13] Shuteng He, Henghui Ding, Xudong Jiang, and Bihan Wen. Segpoint: Segment any point cloud via large language model. *Proceedings of the IEEE/CVF European Conference on Computer Vision*, 2024. 2, 3, 4, 6
- [14] Yining Hong, Haoyu Zhen, Peihao Chen, Shuhong Zheng, Yilun Du, Zhenfang Chen, and Chuang Gan. 3d-llm: Injecting the 3d world into large language models. *Advances in Neural Information Processing Systems*, 36:20482–20494, 2023. 2, 7
- [15] Edward J Hu, Yelong Shen, Phillip Wallis, Zeyuan Allen-Zhu, Yuanzhi Li, Shean Wang, Lu Wang, and Weizhu Chen. Lora: Low-rank adaptation of large language models. *arXiv preprint arXiv:2106.09685*, 2021. 6
- [16] Kuan-Chih Huang, Xiangtai Li, Lu Qi, Shuicheng Yan, and Ming-Hsuan Yang. Reason3d: Searching and reasoning 3d segmentation via large language model. *arXiv preprint arXiv:2405.17427*, 2024. 2, 3, 4, 6
- [17] Pin-Hao Huang, Han-Hung Lee, Hwann-Tzong Chen, and Tyng-Luh Liu. Text-guided graph neural networks for referring 3d instance segmentation. In *Proceedings of the AAAI Conference on Artificial Intelligence*, pages 1610–1618, 2021. 2
- [18] Shijia Huang, Yilun Chen, Jiaya Jia, and Liwei Wang. Multi-view transformer for 3d visual grounding. In *Proceedings of the IEEE/CVF Conference on Computer Vision and Pattern Recognition*, pages 15524–15533, 2022. 2
- [19] Zhening Huang, Xiaoyang Wu, Xi Chen, Hengshuang Zhao, Lei Zhu, and Joan Lasenby. Openins3d: Snap and lookup for 3d open-vocabulary instance segmentation. *arXiv preprint arXiv:2309.00616*, 2023. 2
- [20] Weitai Kang, Mengxue Qu, Jyoti Kini, Yunchao Wei, Mubarak Shah, and Yan Yan. Intent3d: 3d object detection in rgb-d scans based on human intention. *arXiv preprint arXiv:2405.18295*, 2024. 2
- [21] Amrin Kareem, Jean Lahoud, and Hisham Cholakkal. Paris3d: Reasoning-based 3d part segmentation using large

multimodal model. *Proceedings of the IEEE/CVF European Conference on Computer Vision*, 2024. 3

[22] Diederik P Kingma. Adam: A method for stochastic optimization. *International Conference on Learning Representations*, 2015. 6

[23] Xin Lai, Zhuotao Tian, Yukang Chen, Yanwei Li, Yuhui Yuan, Shu Liu, and Jiaya Jia. Lisa: Reasoning segmentation via large language model. In *Proceedings of the IEEE/CVF Conference on Computer Vision and Pattern Recognition*, pages 9579–9589, 2024. 2, 3, 6

[24] Junnan Li, Dongxu Li, Silvio Savarese, and Steven Hoi. Blip-2: Bootstrapping language-image pre-training with frozen image encoders and large language models. In *International Conference on Machine Learning*, pages 19730–19742. PMLR, 2023. 3

[25] Haotian Liu, Chunyuan Li, Qingyang Wu, and Yong Jae Lee. Visual instruction tuning. *Advances in Neural Information Processing Systems*, 36, 2023. 2, 3

[26] Kunhao Liu, Fangneng Zhan, Jiahui Zhang, Muyu Xu, Yingchen Yu, Abdulmotaleb El Saddik, Christian Theobalt, Eric Xing, and Shijian Lu. Weakly supervised 3d open-vocabulary segmentation. *Advances in Neural Information Processing Systems*, 36:53433–53456, 2023. 2

[27] Xiaojian Ma, Silong Yong, Zilong Zheng, Qing Li, Yitao Liang, Song-Chun Zhu, and Siyuan Huang. Sqa3d: Situated question answering in 3d scenes. *International Conference on Learning Representations*, 2023. 2

[28] Fausto Milletari, Nassir Navab, and Seyed-Ahmad Ahmadi. V-net: Fully convolutional neural networks for volumetric medical image segmentation. In *2016 fourth international conference on 3D vision*, pages 565–571. Ieee, 2016. 6

[29] Phuc DA Nguyen, Tuan Duc Ngo, Chuang Gan, Evangelos Kalogerakis, Anh Tran, Cuong Pham, and Khoi Nguyen. Open3dis: Open-vocabulary 3d instance segmentation with 2d mask guidance. *Proceedings of the IEEE/CVF Conference on Computer Vision and Pattern Recognition*, 2024. 2

[30] Maria Parelli, Alexandros Delitzas, Nikolas Hars, Georgios Vlassis, Sotirios Anagnostidis, Gregor Bachmann, and Thomas Hofmann. Clip-guided vision-language pre-training for question answering in 3d scenes. In *Proceedings of the IEEE/CVF Conference on Computer Vision and Pattern Recognition*, pages 5607–5612, 2023. 2

[31] Songyou Peng, Kyle Genova, Chiyou Jiang, Andrea Tagliasacchi, Marc Pollefeys, Thomas Funkhouser, et al. Openscene: 3d scene understanding with open vocabularies. In *Proceedings of the IEEE/CVF Conference on Computer Vision and Pattern Recognition*, pages 815–824, 2023. 2, 6, 7

[32] Renjie Pi, Jiahui Gao, Shizhe Diao, Rui Pan, Hanze Dong, Jipeng Zhang, Lewei Yao, Jianhua Han, Hang Xu, Lingpeng Kong, et al. Detgpt: Detect what you need via reasoning. *Conference on Empirical Methods in Natural Language Processing*, 2023. 3

[33] Zhipeng Qian, Yiwei Ma, Jiayi Ji, and Xiaoshuai Sun. X-refseg3d: Enhancing referring 3d instance segmentation via structured cross-modal graph neural networks. In *Proceedings of the AAAI Conference on Artificial Intelligence*, pages 4551–4559, 2024. 2

[34] Zhongwei Ren, Zhicheng Huang, Yunchao Wei, Yao Zhao, Dongmei Fu, Jiashi Feng, and Xiaojie Jin. Pixellm: Pixel reasoning with large multimodal model. In *Proceedings of the IEEE/CVF Conference on Computer Vision and Pattern Recognition*, pages 26374–26383, 2024. 2, 3, 6

[35] David Rozenberszki, Or Litany, and Angela Dai. Language-grounded indoor 3d semantic segmentation in the wild. In *Proceedings of the IEEE/CVF European Conference on Computer Vision*, pages 125–141. Springer, 2022. 3

[36] Ayça Takmaz, Elisabetta Fedele, Robert W Sumner, Marc Pollefeys, Federico Tombari, and Francis Engelmann. Open-mask3d: Open-vocabulary 3d instance segmentation. *Advances in Neural Information Processing Systems*, 2023. 2

[37] Hugo Touvron, Thibaut Lavril, Gautier Izacard, Xavier Martinet, Marie-Anne Lachaux, Timothée Lacroix, Baptiste Rozière, Naman Goyal, Eric Hambro, Faisal Azhar, et al. Llama: Open and efficient foundation language models. *arXiv preprint arXiv:2302.13971*, 2023. 6

[38] Junchi Wang and Lei Ke. Llm-seg: Bridging image segmentation and large language model reasoning. In *Proceedings of the IEEE/CVF Conference on Computer Vision and Pattern Recognition*, pages 1765–1774, 2024. 2, 3, 6

[39] Wenhui Wang, Zhe Chen, Xiaokang Chen, Jiannan Wu, Xizhou Zhu, Gang Zeng, Ping Luo, Tong Lu, Jie Zhou, Yu Qiao, et al. Visionllm: Large language model is also an open-ended decoder for vision-centric tasks. *Advances in Neural Information Processing Systems*, 36, 2023. 3

[40] Changli Wu, Yihang Liu, Jiayi Ji, Yiwei Ma, Haowei Wang, Gen Luo, Henghui Ding, Xiaoshuai Sun, and Rongrong Ji. 3d-gres: Generalized 3d referring expression segmentation. *Proceedings of the ACM International Conference on Multimedia*, 2024. 2, 7

[41] Changli Wu, Yiwei Ma, Qi Chen, Haowei Wang, Gen Luo, Jiayi Ji, and Xiaoshuai Sun. 3d-stmn: Dependency-driven superpoint-text matching network for end-to-end 3d referring expression segmentation. In *Proceedings of the AAAI Conference on Artificial Intelligence*, pages 5940–5948, 2024. 2, 7

[42] Jannan Wu, Muyan Zhong, Sen Xing, Zeqiang Lai, Zhaoyang Liu, Wenhui Wang, Zhe Chen, Xizhou Zhu, Lewei Lu, Tong Lu, et al. Visionllm v2: An end-to-end generalist multimodal large language model for hundreds of vision-language tasks. *arXiv preprint arXiv:2406.08394*, 2024. 3

[43] Cilin Yan, Haochen Wang, Shilin Yan, Xiaolong Jiang, Yao Hu, Guoliang Kang, Weidi Xie, and Efstratios Gavves. Visa: Reasoning video object segmentation via large language models. *Proceedings of the IEEE/CVF European Conference on Computer Vision*, 2024. 3, 6

[44] Mi Yan, Jiazhao Zhang, Yan Zhu, and He Wang. Maskclustering: View consensus based mask graph clustering for open-vocabulary 3d instance segmentation. *Proceedings of the IEEE/CVF Conference on Computer Vision and Pattern Recognition*, 2024. 2

[45] Jianing Yang, Xuwei Chen, Shengyi Qian, Nikhil Madaan, Madhavan Iyengar, David F Fouhey, and Joyce Chai. Llm-grounder: Open-vocabulary 3d visual grounding with large language model as an agent. In *International Conference on Robotics and Automation*, pages 7694–7701. IEEE, 2024. 2

[46] Jihan Yang, Runyu Ding, Weipeng Deng, Zhe Wang, and Xiaojuan Qi. Regionplc: Regional point-language contrastive learning for open-world 3d scene understanding. In *Proceedings of the IEEE/CVF Conference on Computer Vision and Pattern Recognition*, pages 19823–19832, 2024. [2](#), [6](#), [7](#)

[47] Yuqi Yang, Peng-Tao Jiang, Jing Wang, Hao Zhang, Kai Zhao, Jinwei Chen, and Bo Li. Empowering segmentation ability to multi-modal large language models. *arXiv preprint arXiv:2403.14141*, 2024. [2](#)

[48] Qinghao Ye, Haiyang Xu, Guohai Xu, Jiabo Ye, Ming Yan, Yiyang Zhou, Junyang Wang, Anwen Hu, Pengcheng Shi, Yaya Shi, et al. mplug-owl: Modularization empowers large language models with multimodality. *arXiv preprint arXiv:2304.14178*, 2023. [3](#)

[49] Zhihao Yuan, Xu Yan, Yinghong Liao, Ruimao Zhang, Sheng Wang, Zhen Li, and Shuguang Cui. Instancerefer: Cooperative holistic understanding for visual grounding on point clouds through instance multi-level contextual referring. In *Proceedings of the IEEE/CVF International Conference on Computer Vision*, pages 1791–1800, 2021. [2](#)

[50] Hang Zhang, Xin Li, and Lidong Bing. Video-llama: An instruction-tuned audio-visual language model for video understanding. *Conference on Empirical Methods in Natural Language Processing*, 2023. [3](#)

[51] Shilong Zhang, Peize Sun, Shoufa Chen, Min Xiao, Wenqi Shao, Wenwei Zhang, Yu Liu, Kai Chen, and Ping Luo. Gpt4roi: Instruction tuning large language model on region-of-interest. *arXiv preprint arXiv:2307.03601*, 2023. [3](#)

[52] Deyao Zhu, Jun Chen, Xiaoqian Shen, Xiang Li, and Mohamed Elhoseiny. Minigpt-4: Enhancing vision-language understanding with advanced large language models. *International Conference on Learning Representations*, 2024. [3](#)

[53] Ziyu Zhu, Xiaojian Ma, Yixin Chen, Zhidong Deng, Siyuan Huang, and Qing Li. 3d-vista: Pre-trained transformer for 3d vision and text alignment. In *Proceedings of the IEEE/CVF International Conference on Computer Vision*, pages 2911–2921, 2023. [2](#), [7](#)